AEDC-TN-58-72

(TITLE UNCLASSIFIED)

AERODYNAMIC TEST RESULTS OF TWO CONFIGURATIONS OF A PROPOSED BOMBER DEFENSE MISSILE AT SUPERSONIC SPEEDS

By
Adrian Anderson
GDF, ARO, Inc

October 1958

ARNOLD ENGINEERING DEVELOPMENT CENTER
AIR RESEARCH AND DEVELOPMENT COMMAND
US AF

(Title Unclassified)

AERODYNAMIC TEST RESULTS OF TWO CONFIGURATIONS OF A PROPOSED BOMBER DEFENSE MISSILE AT SUPERSONIC SPEEDS

This document contains matter of a proprietary nature. Its distribution should be limited to the US Military Establishment; other distribution subject to approval of Headquarters, Arnold Engineering Development Center.

By

Adrian Anderson

GDF, ARO, Inc.

October 1958

ARO Project No. 311834

Contract No. AF 40(600)-700 S/A 13(59-1)

CONTENTS

	Page
ABSTRACT	4
NOMENCLATURE	4
INTRODUCTION	5
TEST DESCRIPTION	5
Wind Tunnel	5
Models	5
Instrumentation	6
TEST PROCEDURE	6
DATA REDUCTION	7
PRECISION OF DATA	7
RESULTS	8

ILLUSTRATIONS

Figure

1. General Arrangement of Tunnel E-1 10

2. Photographs of Model I in Tunnel E-1
   a. Transition Roughness at Mid Chord 11
   b. Transition Roughness at Leading-Edge 12

3. Sketches of Models 13

4. Sketch of Model and Balance Arrangement 14

5. Force and Moment Coefficients vs Angle of Attack, Model I
   a. M = 3.00 15
   b. M = 3.98 16
   c. M = 5.00 17

6. Force and Moment Coefficients vs Angle of Attack, Model II
   a. M = 3.00 18
   b. M = 3.98 19
   c. M = 5.00 20

7. Center-of-Pressure Locations at Angle of Attack . 21

8. Drag Coefficients vs Reynolds Number at Mach 3.0, $\alpha = 0^{o}$ 22

9. Drag Coefficients vs Reynolds Number at Mach 5.0, $\alpha = 0^{o}$ 23

Figure		Page
10.	Schlieren Pictures of Model I at Mach 3.0	
	a. Model Clean, R = 3 x 10^6	24
	b. Roughness at Leading-Edge, R = 1 x 10^6	24
	c. Roughness at Mid-Chord, R = 1.04 x 10^6	24
	d. Roughness at Mid-Chord, R = 1.48 x 10^6	25
	e. Roughness at Mid-Chord, R = 3 x 10^6	25
11.	Schlieren Pictures of Model II at Mach 3.0; R = 1.6 x 10^6	
	a. Model Clean	26
	b. Roughness at Mid-Chord	26
	c. Roughness at Leading-Edge	26
12.	Schlieren Pictures of Model I at Mach 5.0	
	a. Model Clean, R = 2.23 x 10^6	27
	b. Roughness at Leading-Edge, R = 1.29 x 10^6	27
	c. Roughness at Leading-Edge, R = 1.66 x 10^6	28
	d. Roughness at Leading-Edge, R = 2.02 x 10^6	28

ABSTRACT

Two configurations of a proposed bomber defense missile were tested in Tunnel E-1 of the Gas Dynamics Facility, Arnold Engineering Development Center. Force and moment coefficients were obtained at Mach numbers 3.0, 3.98, and 5.0 over an angle-of-attack range from about -5 to 15 deg, with the Reynolds number held essentially constant at 1.50×10^6. In addition, the variations of the forebody and base drag coefficients with Reynolds number were obtained at Mach numbers 3.0 and 5.0 at zero angle of attack over a Reynolds number range from $0.4 - 3.0 \times 10^6$.

NOMENCLATURE

A_b	Model base area, 0.5185 sq in.
c	Model centerline chord, 8.0 in.
C_D	Forebody drag coefficient, $C_{D_T} - C_{D_B}$
C_{D_B}	Base drag coefficient, $(p - p_b)\frac{A_b}{qS}$
C_{D_T}	Total drag coefficient, $\frac{T \cos \alpha + N \sin \alpha}{qS}$
C_L	Lift coefficient, $\frac{N \cos \alpha - T \sin \alpha}{qS}$
C_m	Pitching moment coefficient, M_y/qSc
C_N	Normal force coefficient, N/qS
M	Free-stream Mach number
N	Normal force, lb
p	Free-stream static pressure, psia
p_b	Base pressure, psia
p_o	Stagnation pressure, psia
q	Free-stream dynamic pressure, psia
R	Reynolds number based on model length of 8 in.
S	Model planform area, 50.27 sq in.
T	Axial force, lb
T_o	Stagnation temperature, ^oR
$X_{c,p}$	Distance from center of pressure to model centerline in percent of chord, C_m/C_N (negative aft)
α	Angle of attack, deg

INTRODUCTION

Tests were conducted in Tunnel E-1 of the Gas Dynamics Facility, Arnold Engineering Development Center during the early part of May 1958, at the request of the Technical Planning Group of the Air Proving Ground Center (APGC), Eglin Air Force Base.

The test objective was to provide aerodynamic data on two model configurations required to support an APGC proposal for a bomber defense missile development program.

TEST DESCRIPTION

WIND TUNNEL

Tunnel E-1 is an intermittent, supersonic wind tunnel with a 12-in. by 12-in. test section (Fig. 1). The top and bottom walls of the nozzle are flexible plates which are positioned by screw-jacks to produce any test-section Mach number within the range from 1.5 to 5.0. The allowable stress on the flexible nozzle plate limits the tunnel supply pressure to a maximum of four atmospheres, which is maintained by throttling the flow from a surface-heated, high-pressure, air-storage system. A large vacuum sphere coupled to the downstream end of the tunnel permits operation at low density levels.

MODELS

Two model configurations were tested, one symmetrical (Model I) and the other cambered (Model II). Both the models and sting-support were designed and fabricated by the Eglin APGC to accommodate an existing GDF internal balance. Construction was of aluminum with polished surfaces. Photographs of Model I are given in Fig. 2, and detailed sketches of both models are shown in Figs. 3 and 4.

During the installation of Model I in the tunnel it was decided not to use the "cap" (see Fig. 4) for fairing over the balance locknut cavity because of sealing difficulties. Instead, the locknut cavity was filled with cotton wool and sealed over by a fairing of dental plaster.

Manuscript released by author August 1958.

INSTRUMENTATION

The forces and moments on the models were measured with a six-component internal balance, GDF balance No. E1-B61-15. For these tests, however, only three components were used. The balance design loads on these components are ± 50-lb normal force, ± 22 in.-lb pitching moment, and 10-lb axial force. The gage outputs from the balance were measured with 400-cps force readout units. These units are a null-balance servo system having both a dial indicator and an electrical digitizer serving as the gage input to an ERA 1102 computer.

Absolute base pressure was measured with a 1-psi differential transducer which had essentially a vacuum for a reference pressure. The transducer output was measured with a d-c millivolt digitized recorder which also served as the input to the computer.

A single-pass schlieren system was used to record flow patterns about the models. Other data items such as angle of attack and stagnation temperature and pressure were measured, digitized, and automatically recorded.

TEST PROCEDURE

Force and moment data at angle of attack were obtained for both models at Mach numbers 3.0, 3.98, and 5.0. The test Reynolds number was approximately 1.50×10^6, based on model length of 8 in. The stagnation pressures corresponding to this value of Reynolds number were 40 psia at Mach 5.0, 25 psia at Mach 3.98, and 15 psia at Mach 3.0. Small variations in the test Reynolds number were obtained because the tunnel stagnation temperature during these tests varied within ± 10°F of 90°F.

The stagnation pressure at Mach 5.0 was limited by the allowable loading of the balance, which was critical at the aft-pitch gage section. This limitation also restricted the range of angle of attack at Mach 3.0 and Mach 4.0. The angle of attack at each data point was set manually.

The variation of the drag coefficients with Reynolds number at zero angle of attack was obtained for both models at Mach numbers 3.0 and 5.0. The model and balance were rolled 90 deg from the pitch plane so that schlieren pictures could be made of the flow conditions over the model surfaces. The Reynolds number was varied by varying the stagnation pressure, and again the pressure was limited by the balance loading.

Data were also taken at both Mach numbers with strips of carborundum dust on the models to serve as boundary layer trips. These strips were about one-half inch wide, and two different locations on the model were tried - across the centerline chord and at a position approximately 1-in. aft of the model leading edge. Figure 2 shows these locations.

DATA REDUCTION

The digitized outputs from the internal balance, base pressure, sector angle, stagnation pressure, and stagnation temperature were supplied to the ERA 1102 computer for data reduction. A selected group of data were then plotted in coefficient form on two plotters at the tunnel, and a tabulation of all reduced data was made. Both operations were normally completed within five minutes after each run.

All coefficients are referenced to the wind axes through the moment reference point, and the angles of attack have been corrected for deflections of the sting support due to air loads on the model. The Reynolds number has been computed on the basis of Hirschfelder's approximation for the viscosity of air at temperatures below 216°R.*

PRECISION OF DATA

The estimated uncertainties of the data are given in the following table:

Mach No.	C_L	C_m	C_D	C_{D_B}
3.00	.00071	.00044	.00074	$.10 \times 10^{-4}$
3.98	.00083	.0006	.001	$.051 \times 10^{-4}$
5.00	.00101	.00085	.0011	$.031 \times 10^{-4}$

The uncertainties quoted above were determined from estimates of the uncertainty of the individual measurements which enter into the determination of the quantities. The statistical method used assumes the error distribution of the individual measurements to be normal.** The indicated

---

* Joseph O. Hirschfelder, et al. Molecular Theory of Gases and Liquids. John Wiley and Sons, New York, 1954.

**R. C. Dean, Jr. "Aerodynamic Measurements," Gas Turbine Laboratory, MIT, 1953. (Fourth Printing 1957)

angle of attack is estimated to be accurate to within ±0.1 deg. The test-section Mach numbers are known from calibration to have a maximum variation along the tunnel centerline of ±0.01, with a repeatable accuracy of within ±0.002. No corrections were made for the tunnel airflow angularity which is on the same order as the quoted accuracy of the indicated angle of attack.

RESULTS

The basic force and moment coefficients have been plotted directly against angle of attack and are presented in Figs. 5 and 6.

The forebody drag coefficients for Model I at Mach 5.0 (Fig. 5c) are in error because of difficulties found early in the test program in obtaining a stabilized base pressure. This error is small, however, (less than 1 percent) because the base drag is only a small percentage of the total drag.

On Model II the model camber produced a trim lift coefficient of 0.09 at Mach 3.0, decreasing to 0.05 at Mach 5.0. The corresponding trim angles of attack lie at 5.5 deg and 4.7 deg, respectively. The angle of attack for zero lift was relatively constant, and for all Mach numbers was about 2.0 deg.

A plot of the center of pressure locations as percentages of the centerline chord measured from the leading edge against angle of attack is given in Fig. 7. Included in this figure are, shown in tagged symbols, the neutral point locations as determined for an angle-of-attack range of about three degrees. On both models the neutral point was ahead of the model center, ranging from 14-percent chord for Model II at Mach 3.0 to 19-percent chord for Model I at Mach 5.0.

The variations of the forebody drag and base drag coefficients with Reynolds number for both models at Mach numbers 3.0 and 5.0 are shown in Figs. 8 and 9. These data include the results obtained with strips of carborundum dust on the model surface serving as a boundary layer trip. With the exception of two test runs at Mach 3.0 on Model II where a No. 70 grain size was used, all the roughness strips had a No. 50 grain size.

At Mach 3.0 the boundary layer was tripped on both models with the roughness strip located just aft of the leading edge. The data shows (Fig. 8) that the boundary layer was turbulent over the range of test Reynolds number.

With the roughness at the mid-chord location on Model I, transition did not occur on the model until a Reynolds number of about 1.5 million, at which point transition had moved up along the wake to the base of the model. As Reynolds number was increased, the transition point moved further up on the model; and at the maximum test Reynolds number of 3 million, transition occurred just aft of the roughness strip. This is shown in the data (Fig. 8a) and in the sequence of schlieren pictures in Fig. 10. In Fig. 8a a dashed curve has been drawn through the mid-chord data to indicate the transition region. At Reynolds numbers less than 1 million, the increase in forebody drag coefficient over the model clean (laminar) data may be interpreted as the increase in wave drag from the added roughness. The leading-edge roughness data on both models also includes an unknown amount of added wave drag.

A single layer and a double layer of No. 70 grit size were tested at the mid-chord location on Model II. In neither case was the boundary layer tripped on the model. As the data indicate and as schlieren pictures confirm, the transition point moved up along the wake to the base of the model as Reynolds number increased. The data of Fig. 8b identifies these data together because both cases gave identical results. Schlieren pictures corresponding to the Model II data at a Reynolds number of 1.6 million are given in Fig. 11.

The results at Mach 5.0 on both models (Fig. 9) show that the boundary layer was not tripped and that it was only at the maximum test Reynolds number, with roughness at the leading edge, that turbulent flow was observed on the wake. This is shown in the sequence of schlieren pictures of Model I given in Fig. 12 and by the increase in base drag at this condition. The Model II data show the same condition existing. No base drag data are presented for Model I in the clean condition (Fig. 9a) because of the base pressure errors, mentioned previously. The forebody drag of Model I-clean also includes a small error because of this.

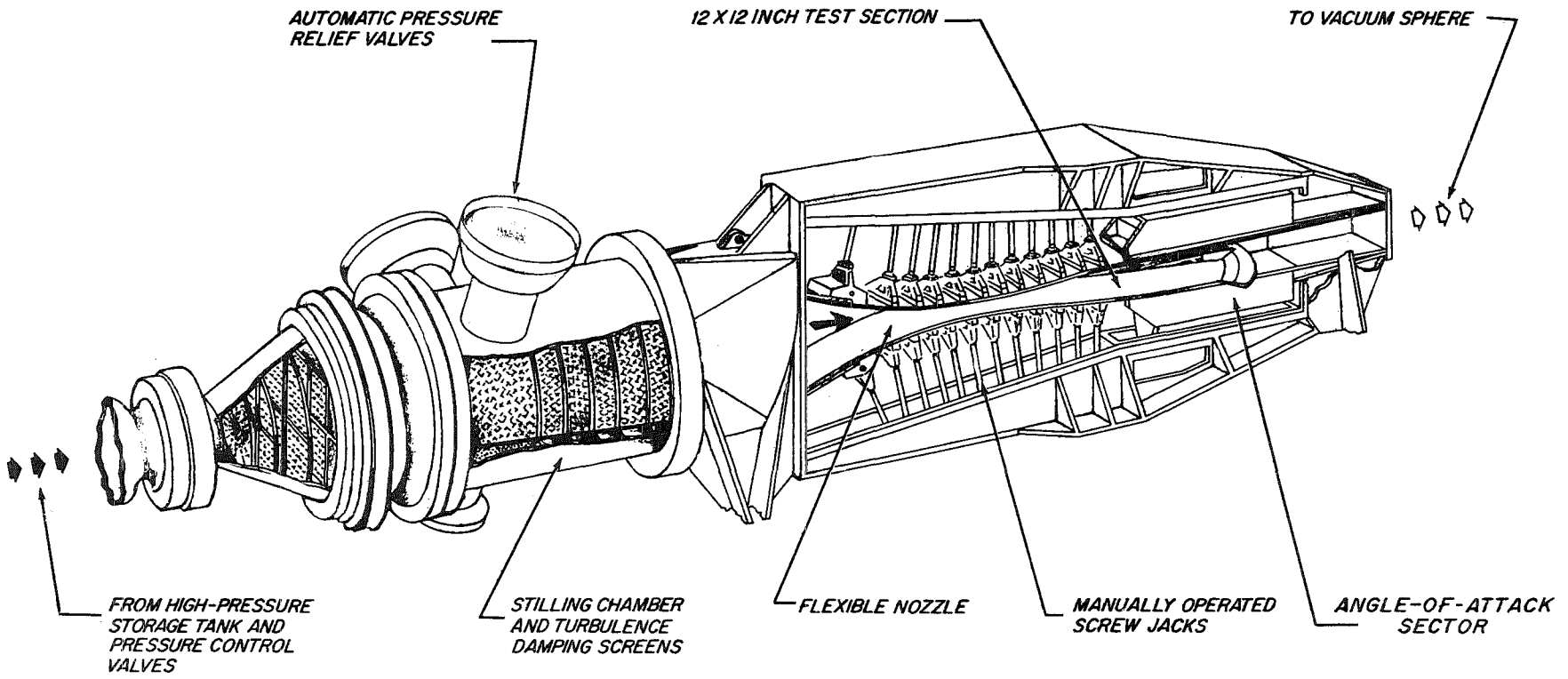

Fig. 1 General Arrangement of Tunnel E-1

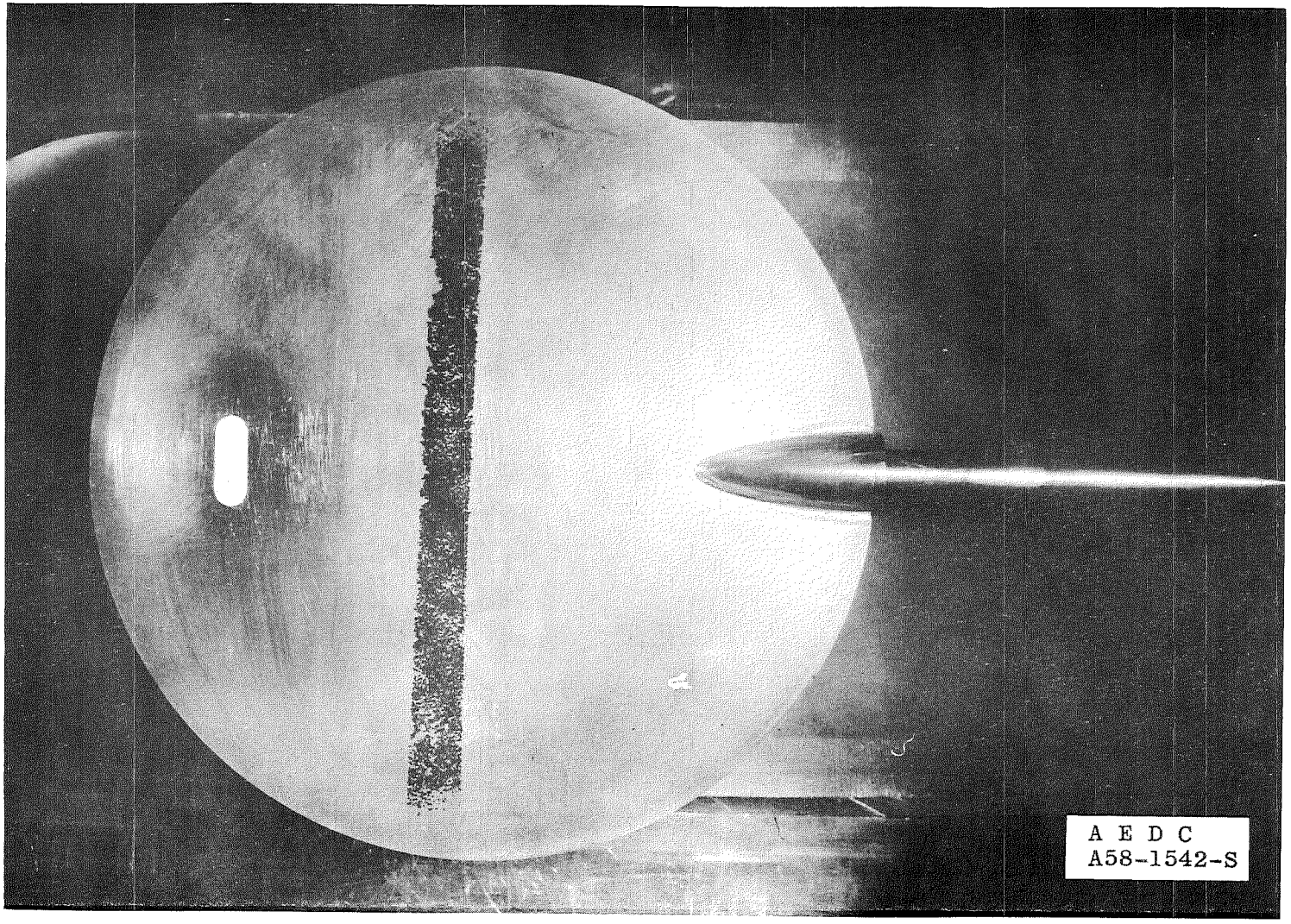

a. Transition Roughness at Mid-Chord

Fig. 2 Photographs of Model I in Tunnel E-1

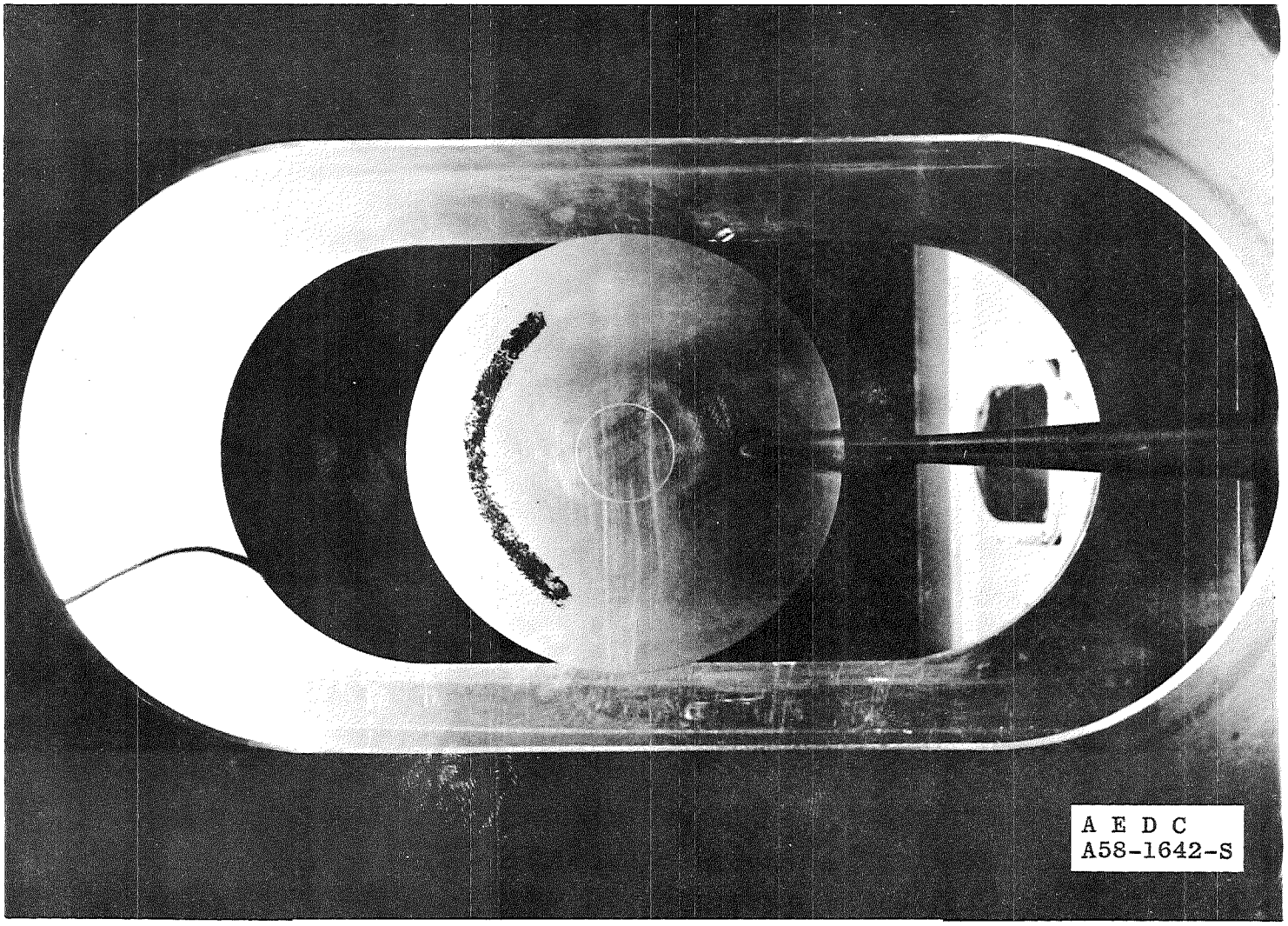

b. Transition Roughness at Leading-Edge

Fig. 2 Concluded

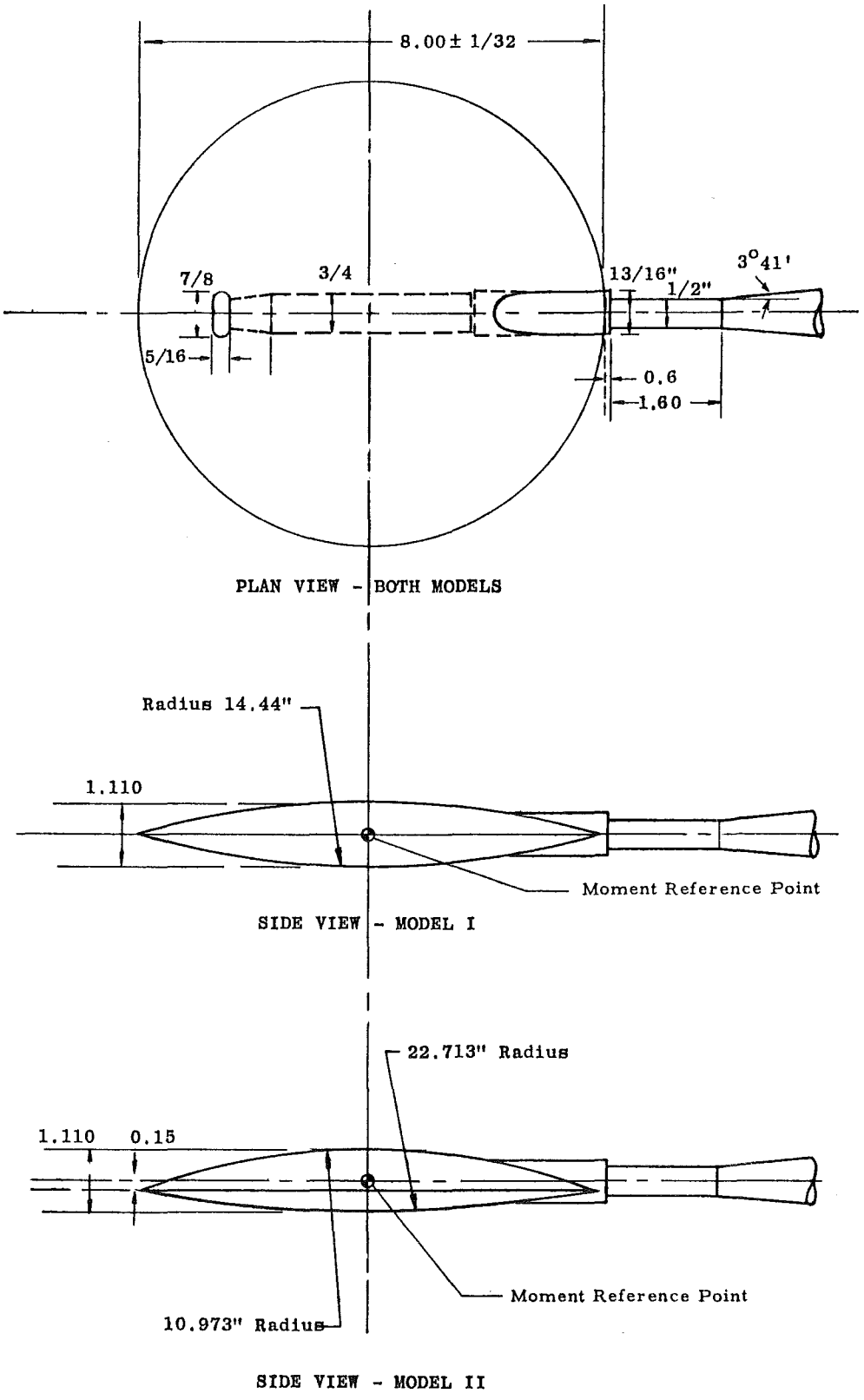

Fig. 3 Sketches of Models

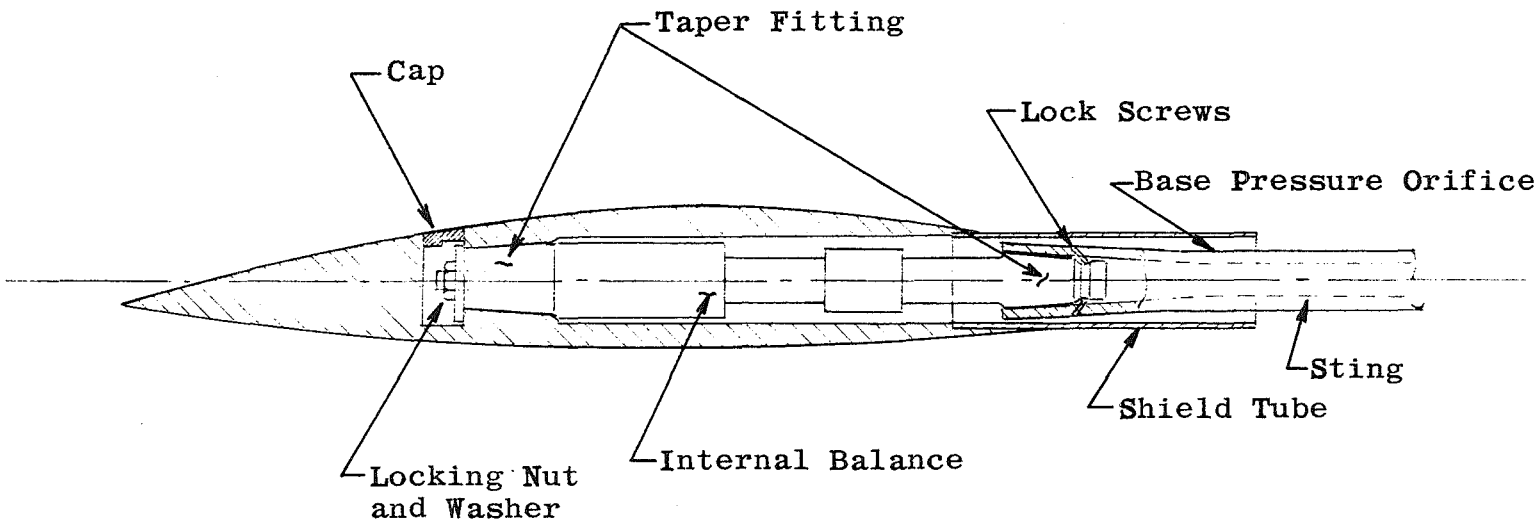

Fig. 4 Sketch of Model and Balance Arrangement

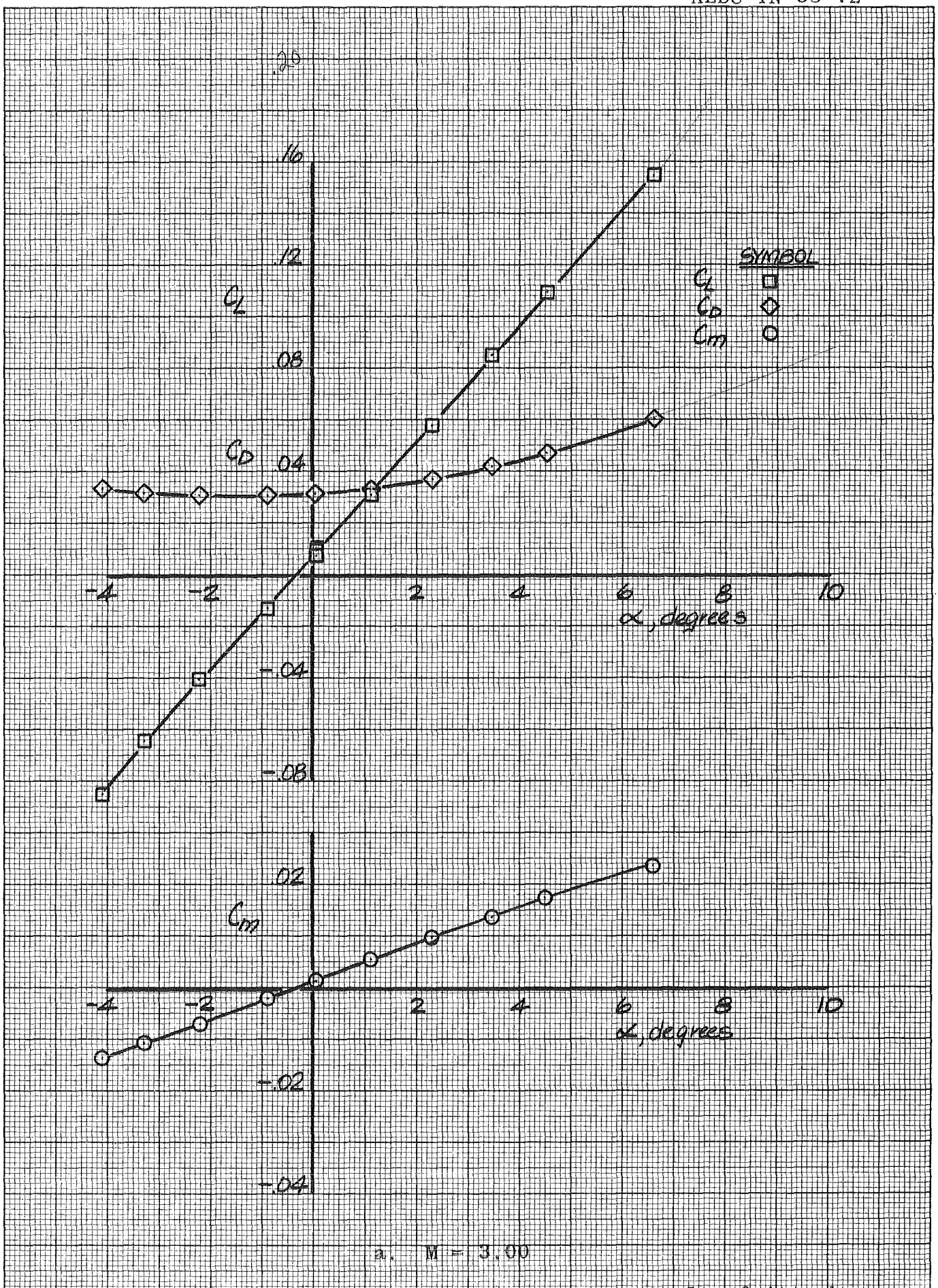

a. M = 3.00

Fig. 5 Force and Moment Coefficients vs Angle of Attack, Model I

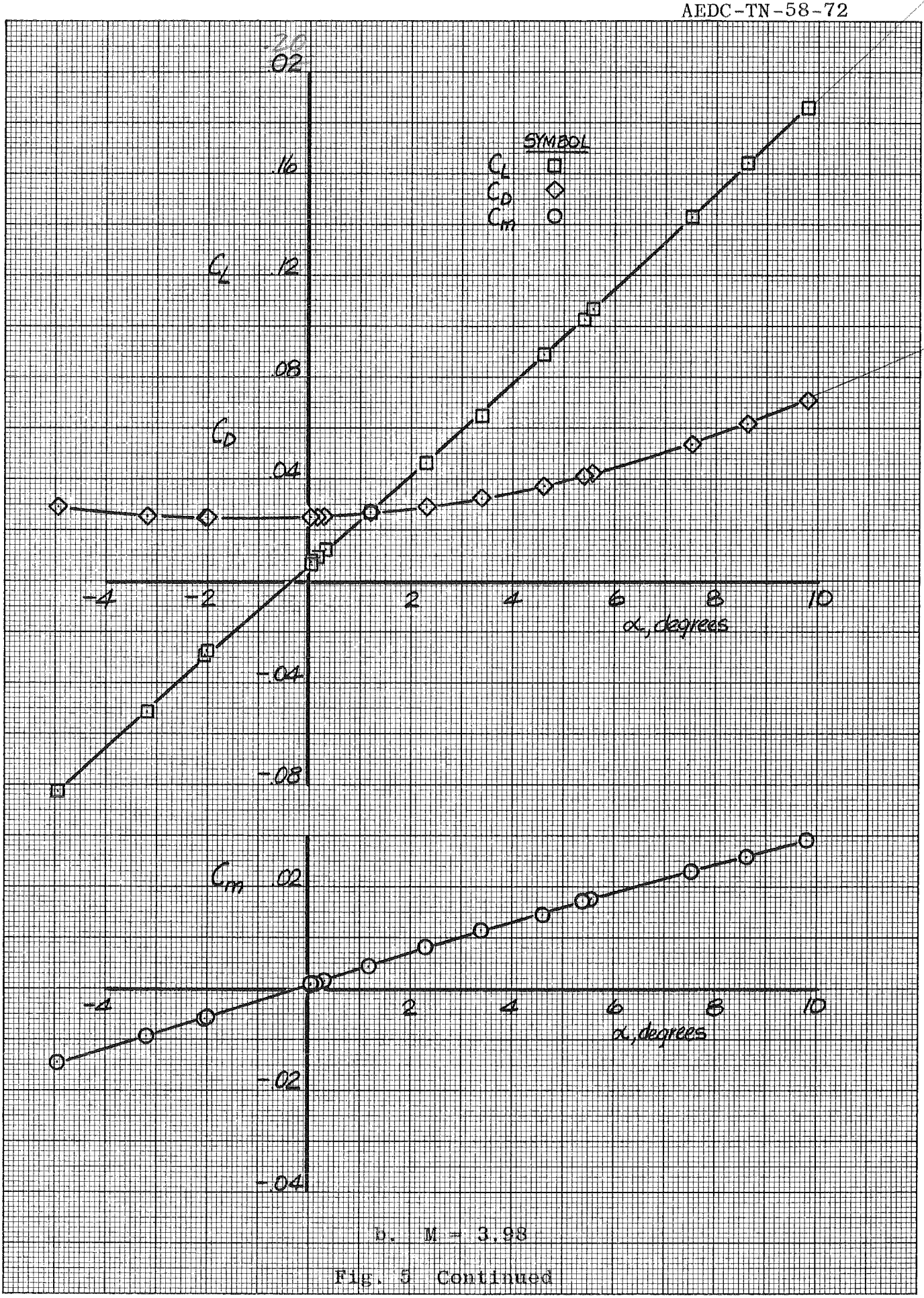

b. M = 3.98

Fig. 5 Continued

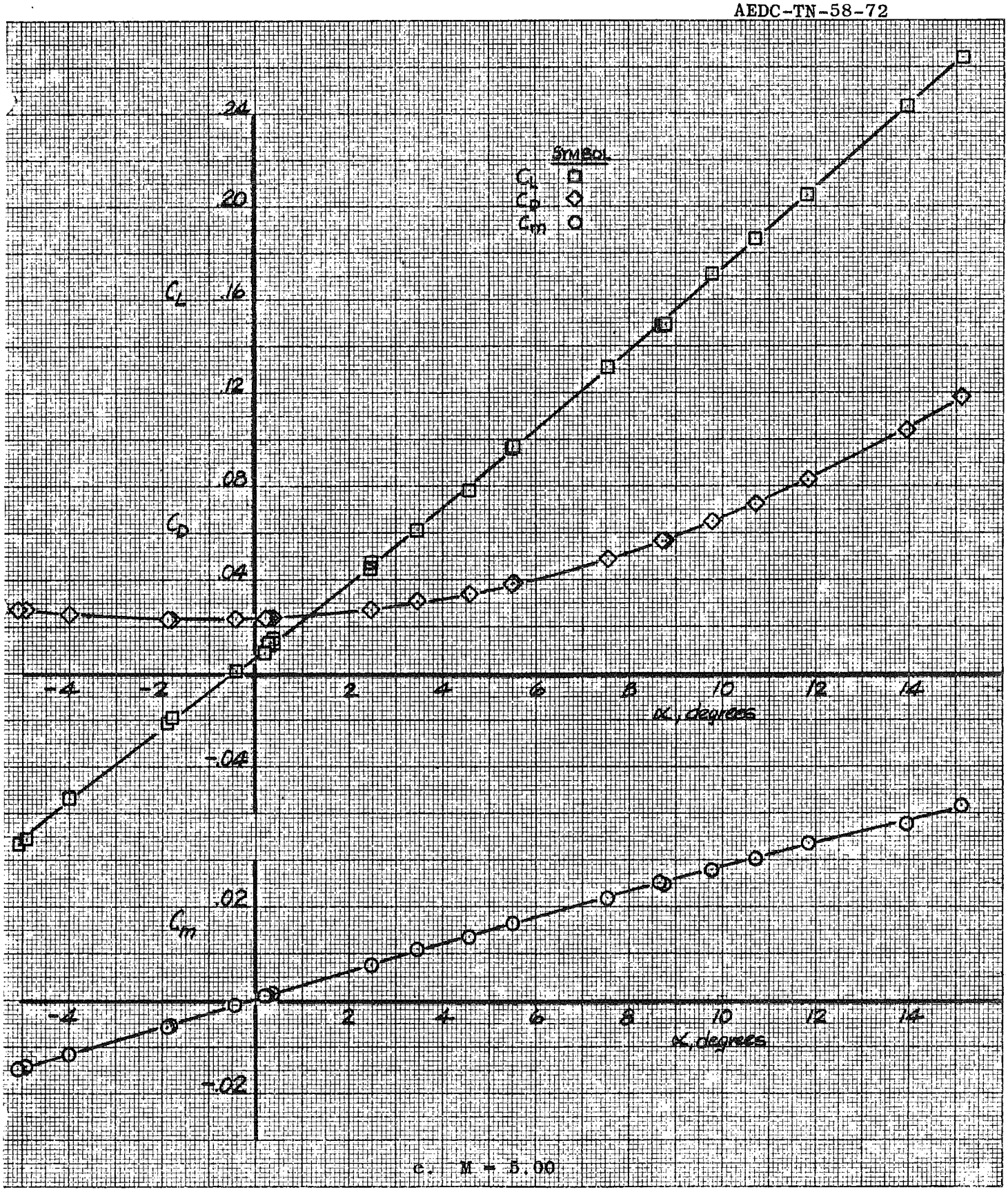

Fig. 5 Concluded

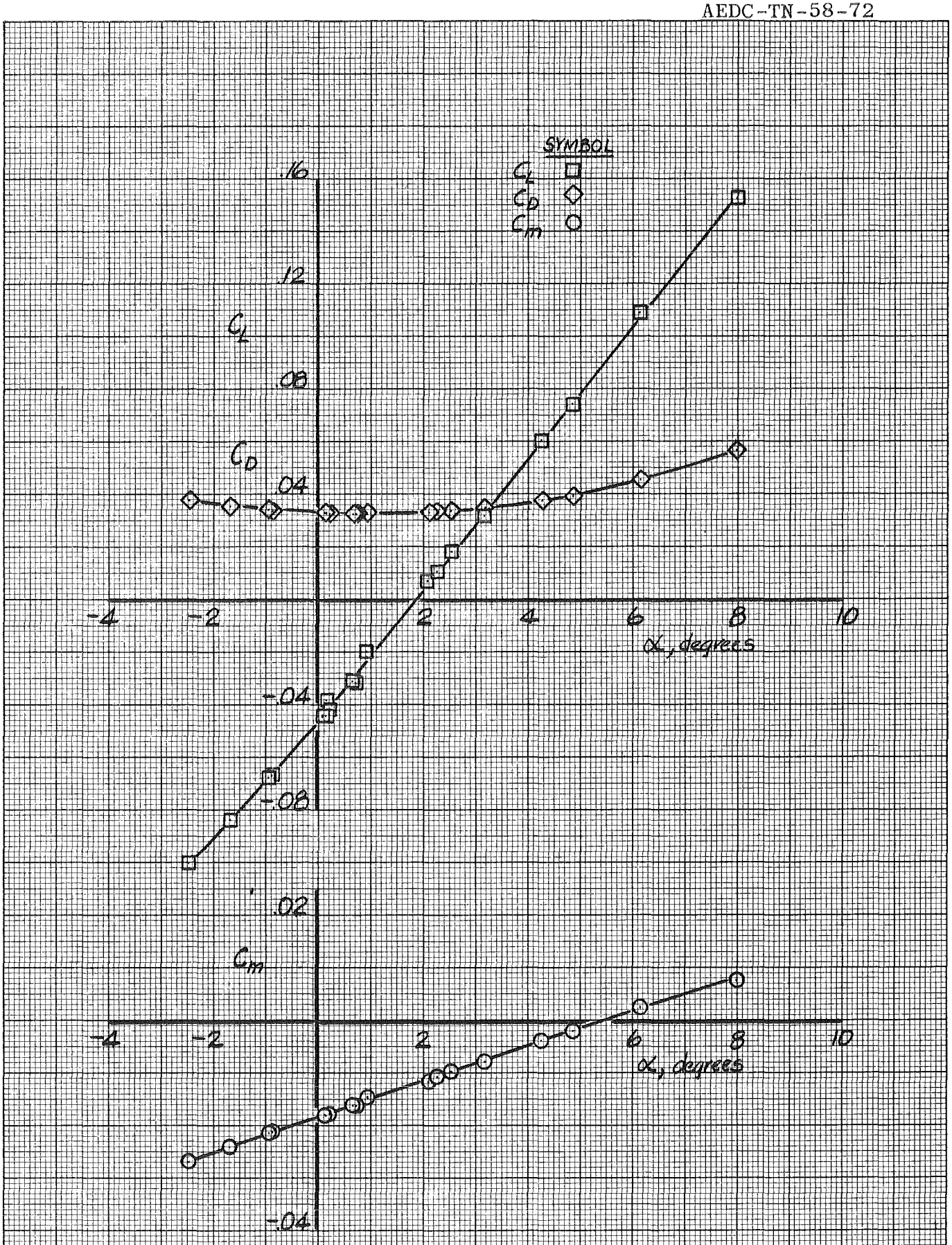

a. M = 3.00

Fig. 6 Force and Moment Coefficients vs Angle of Attack, Model II

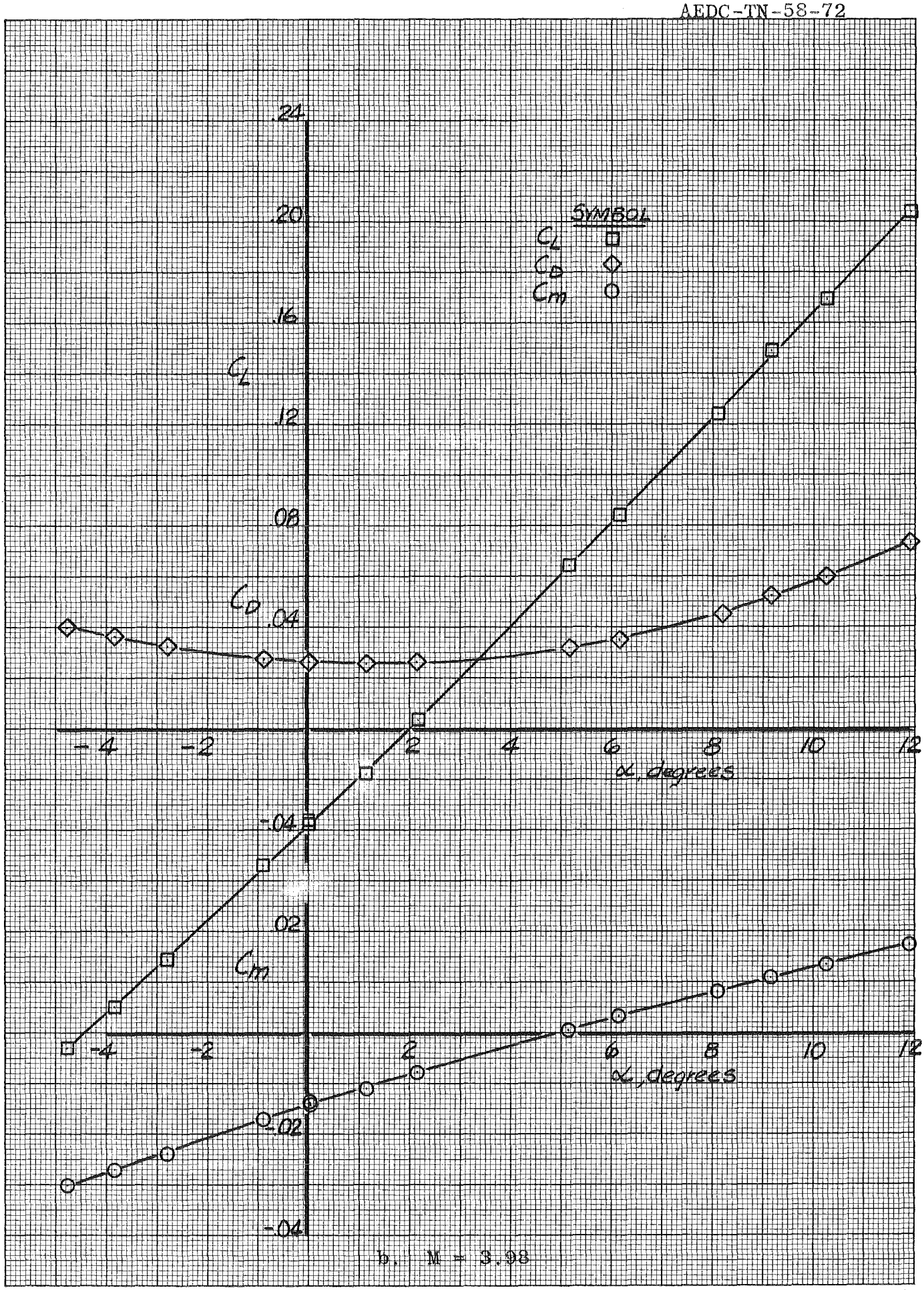

b. M = 3.98

Fig. 6 Continued

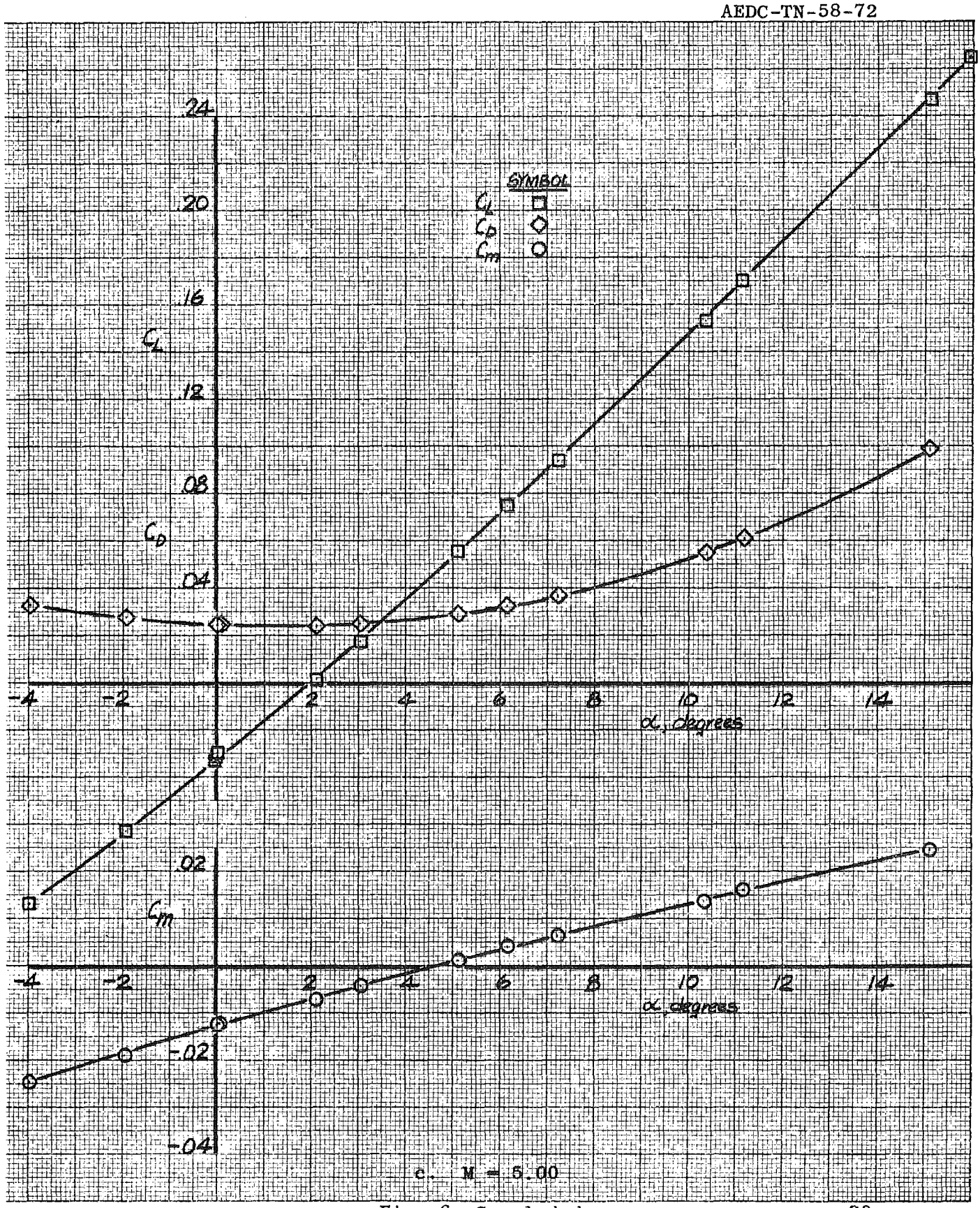

Fig. 6 Concluded

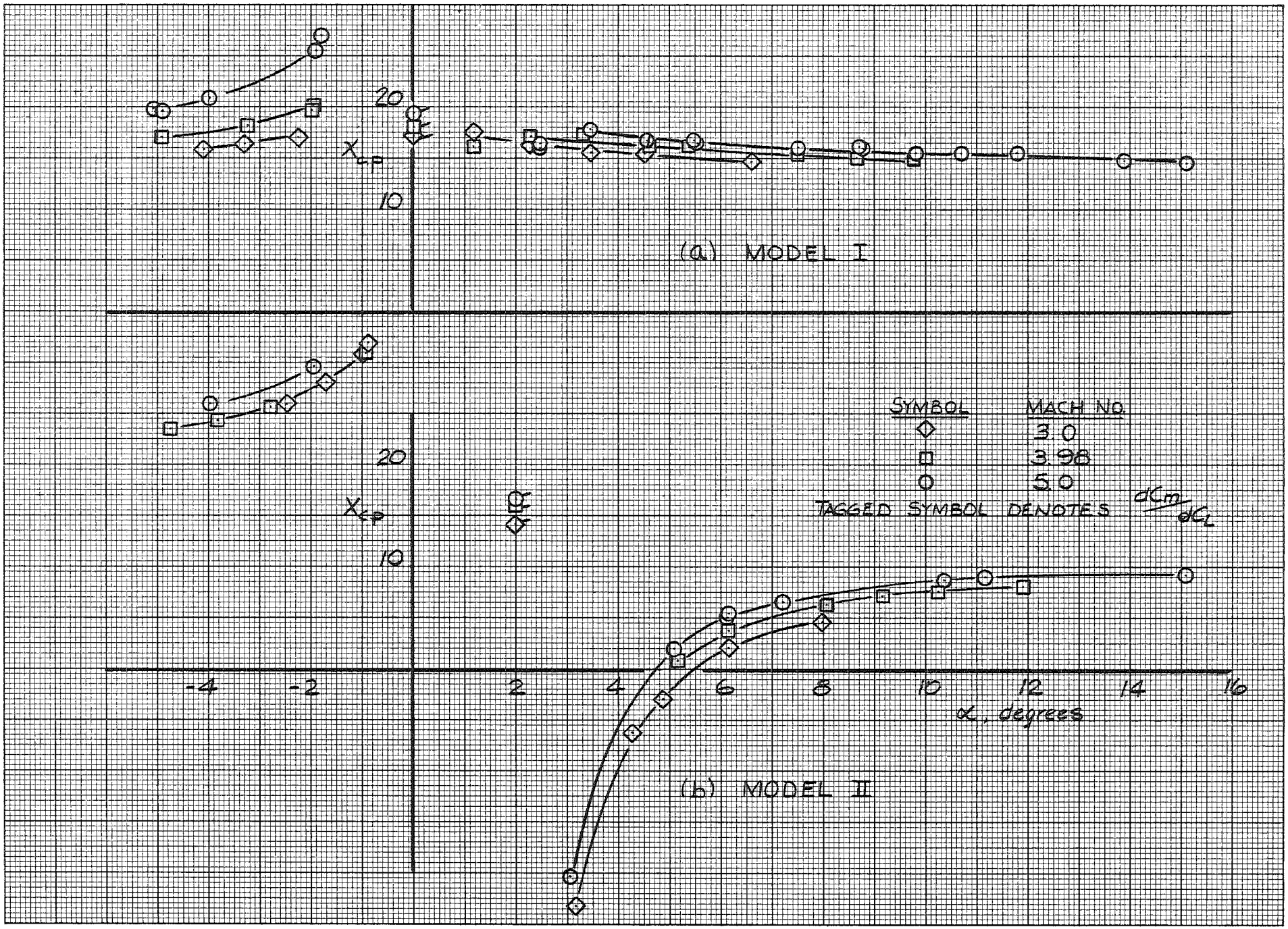

Fig. 7 Center-of-Pressure Locations at Angle of Attack

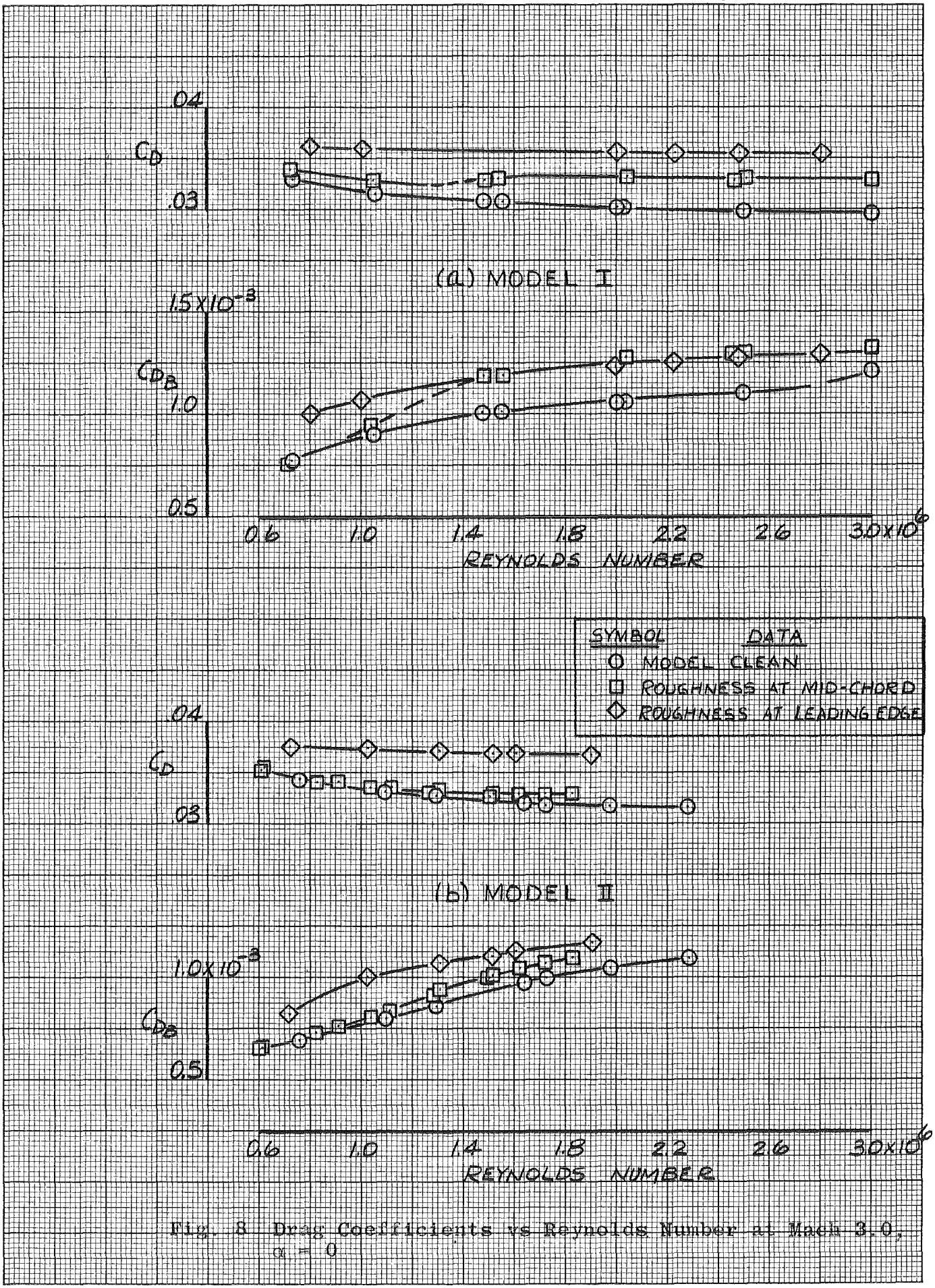

Fig. 8 Drag Coefficients vs Reynolds Number at Mach 3.0, $\alpha = 0$

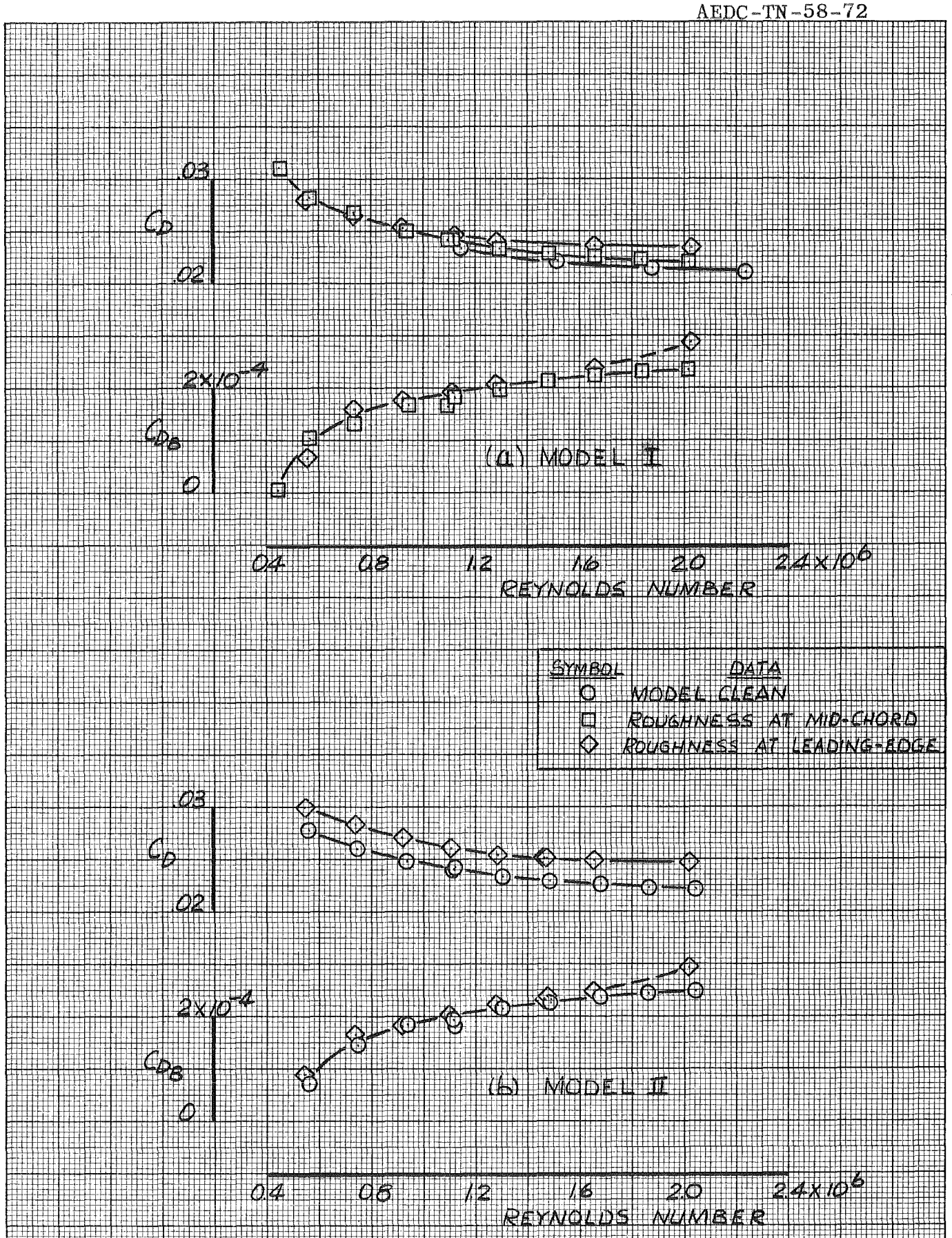

Fig. 9 Drag Coefficients vs Reynolds Number at Mach 5.0, $\alpha = 0$

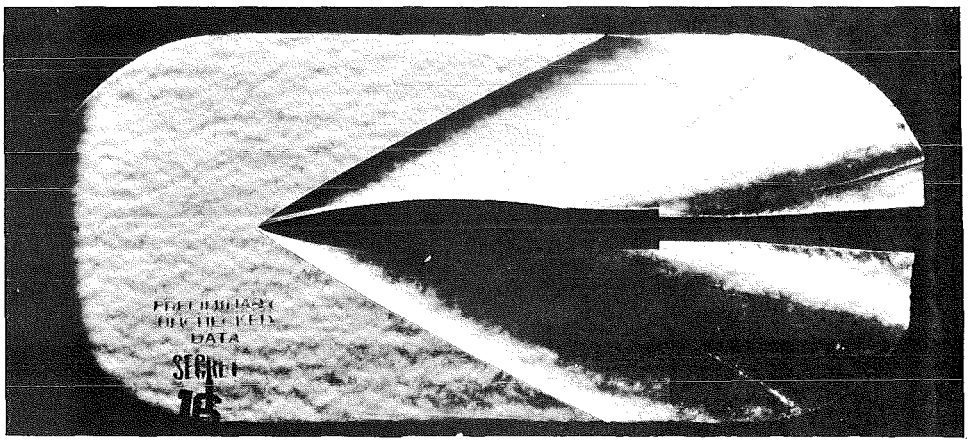

a. Model Clean, $R = 3 \times 10^6$

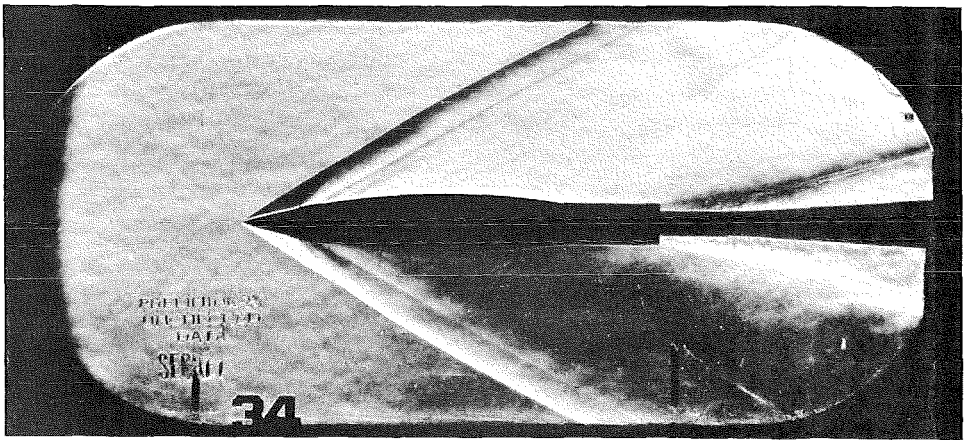

b. Roughness at Leading-Edge, $R = 1 \times 10^6$

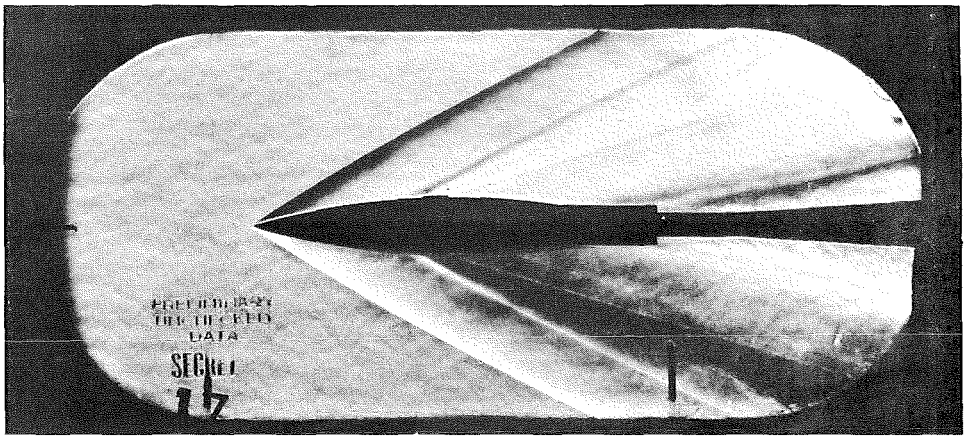

c. Roughness at Mid-Chord, $R = 1.04 \times 10^6$

Fig. 10 Schlieren Pictures of Model I at Mach 3.0

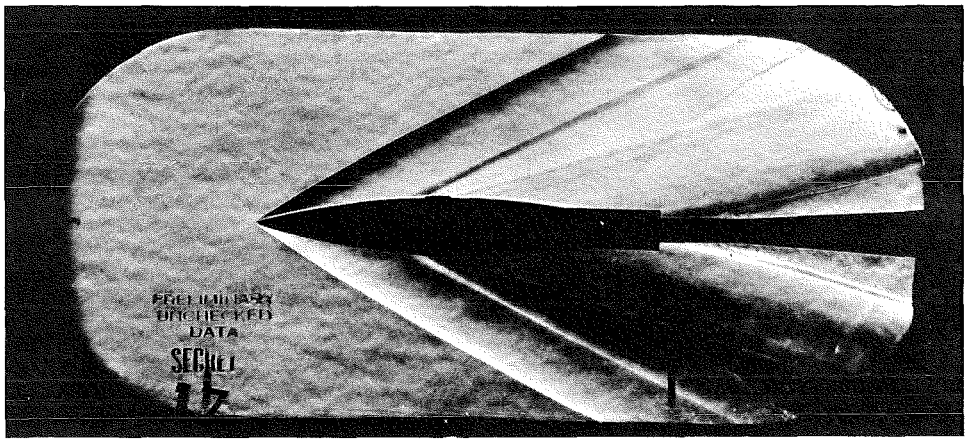

d. Roughness at Mid-Chord, R = 1.48 x 10^6

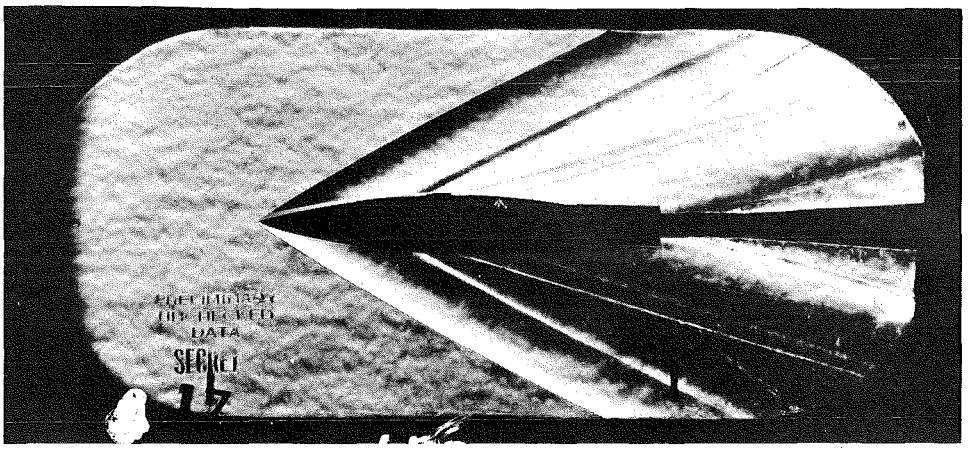

e. Roughness at Mid-Chord, R = 3 x 10^6

Fig. 10 Concluded

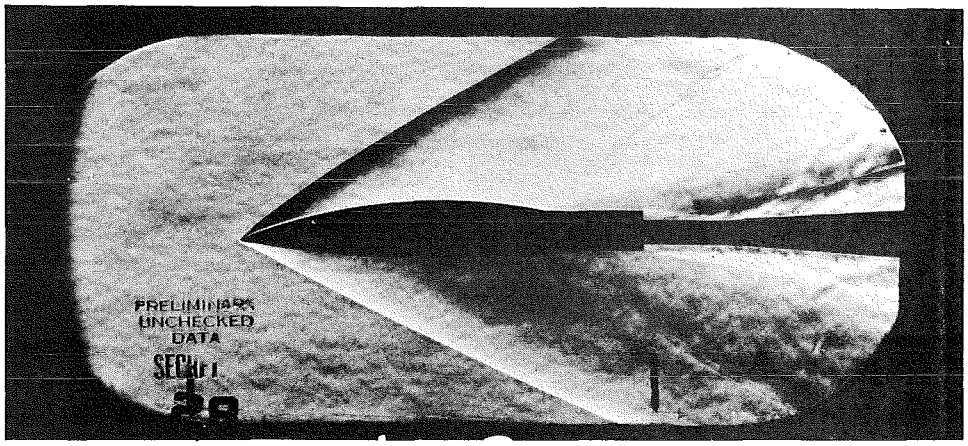

a. Model Clean

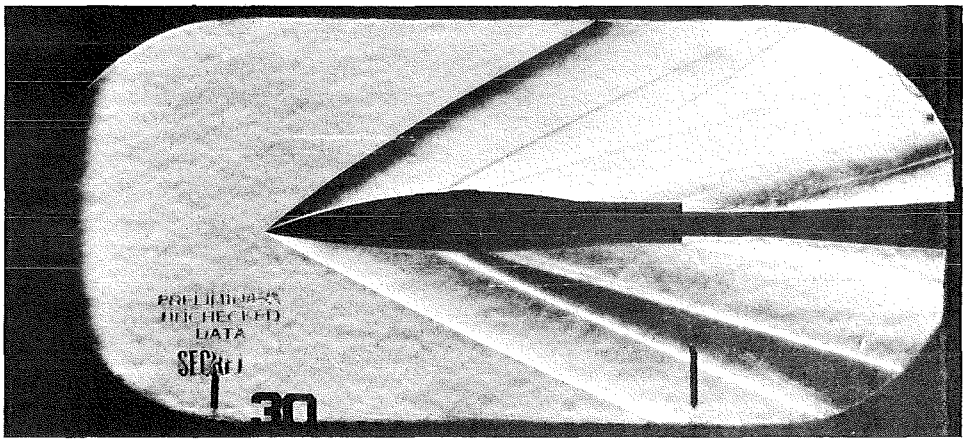

b. Roughness at Mid-Chord

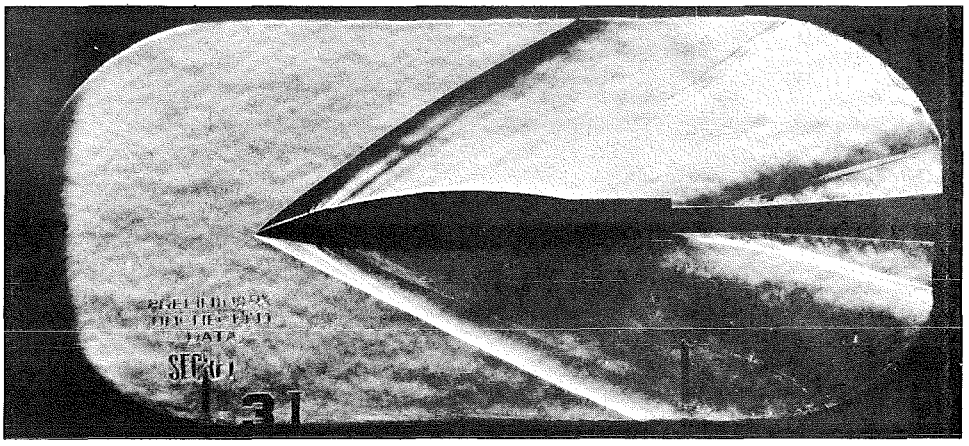

c. Roughness at Leading-Edge

Fig. 11 Schlieren Pictures of Model II at Mach 3.0; $R = 1.6 \times 10^6$

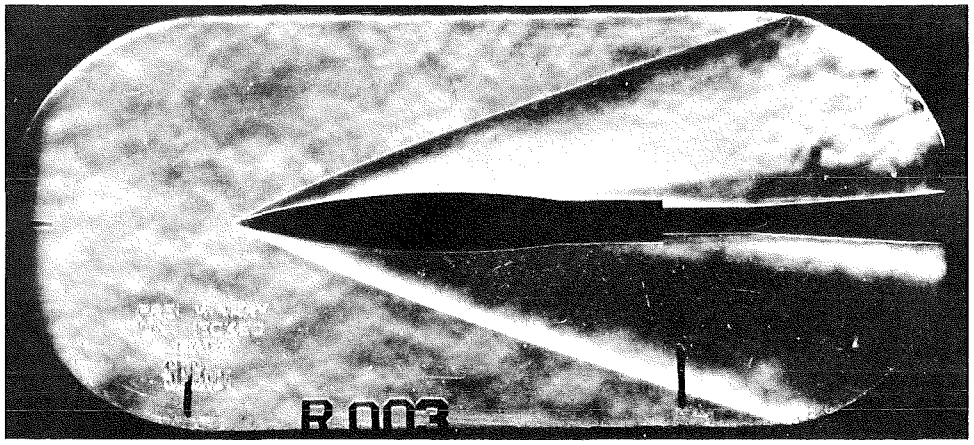

a. Model Clean, $R = 2.23 \times 10^6$

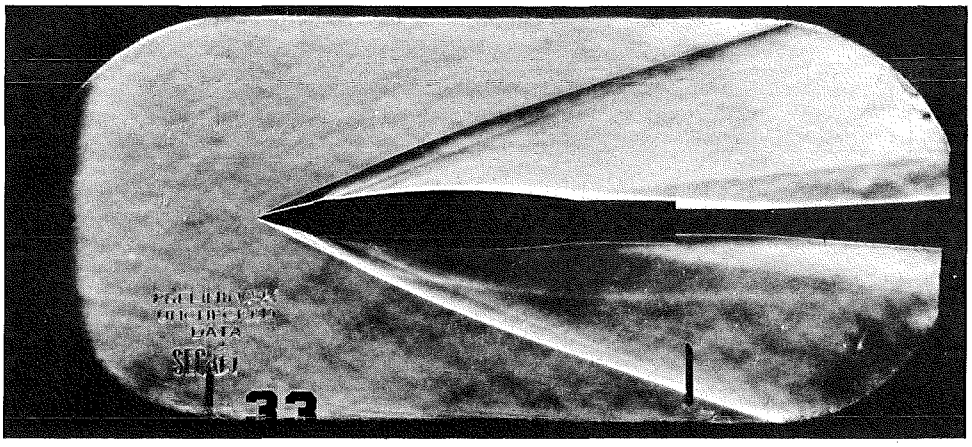

b. Roughness at Leading-Edge, $R = 1.29 \times 10^6$

Fig. 12 Schlieren Pictures of Model I at Mach 5.0

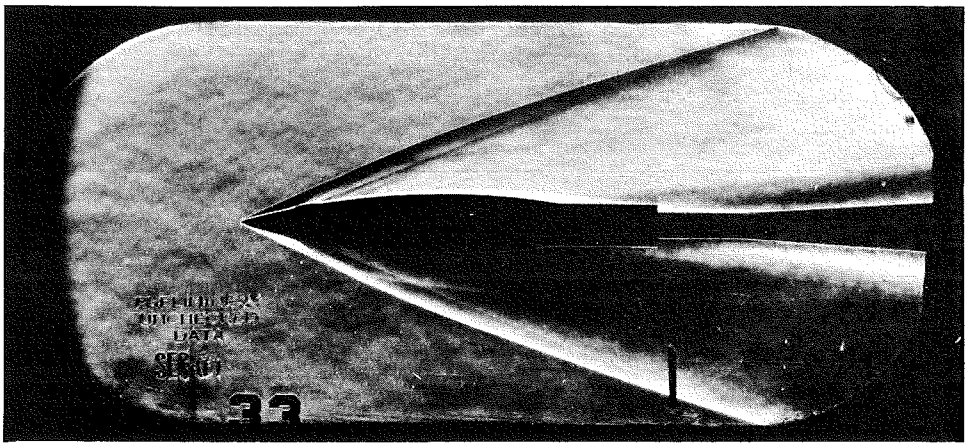

c. Roughness at Leading-Edge, R = 1.66 and 10^6

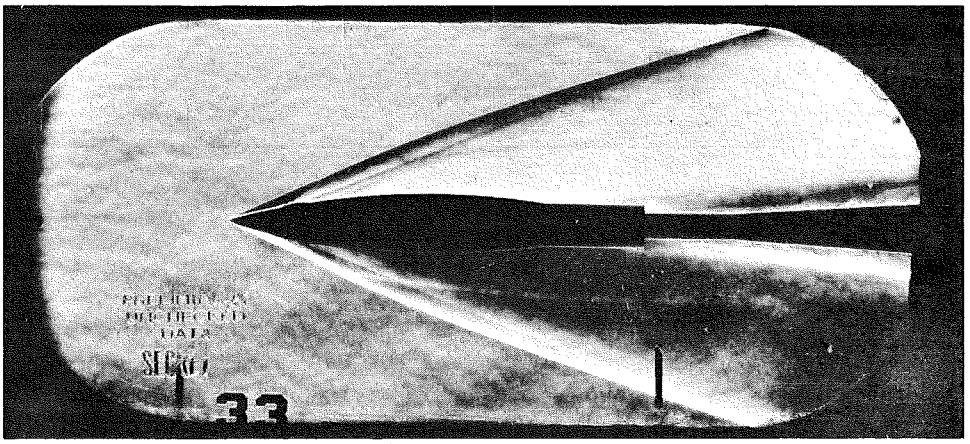

d. Roughness at Leading-Edge, R = 2.02 x 10^6

Fig. 12 Concluded